Analysis of glutamate-dependent mechanism and optimization of fermentation conditions for polyglutamic acid production by Bacillus subtilis SCP017-03

Caiyun Wu
Sichuan Normal University
Yutao Gou
Sichuan Normal University
Shuai Jing
Sichuan Normal University
Wei Li
liwei001@sicnu.edu.cn
Sichuan Normal University
Fanglan Ge
Sichuan Normal University
Jiao Li
Sichuan Normal University
Yao Ren
Sichuan Normal University

Research Article

Keywords: Poly-gamma-glutamic acid, Bacillus subtilis, glutamate-dependent mechanism, transcriptomics and protein omics, fermentation optimization

Posted Date: March 6th, 2024

DOI: https://doi.org/10.21203/rs.3.rs-4005655/v1

Additional Declarations: No competing interests reported.

Abstract

Poly-gamma-glutamic acid (γ-PGA) is mainly synthesized by glutamate-dependent strains in the manufacturing industry. Therefore, understanding glutamate-dependent mechanisms is imperative. In this study, we first systematically analyzed the response of *Bacillus subtilis* SCP017-03 to glutamate addition by comparing transcriptomics and protein genomics. The introduction of glutamate substantially altered the gene expression within the central metabolic pathway of cellular carbon. Most genes in the pentose phosphate pathway (PPP), tricarboxylic acid (TCA) cycle, and energy-consuming phase of the glycolysis pathway (EMP) were down-regulated, whereas genes in the energy-producing phase of glycolysis and those responsible for γ-PGA synthesis were up-regulated. Based on these findings, the fermentation conditions were optimized and the γ-PGA production was improved by incorporating oxygen carriers. In a batch-fed fermentor with glucose, the γ-PGA yield reached 95.2 g/L, demonstrating its industrial production potential. This study not only elucidated the glutamic acid dependence mechanism of *Bacillus subtilis* but also identified a promising metabolic target for further enhancing γ-PGA production.

Introduction

Poly-gamma-glutamic acid (γ-PGA) is a biopolymer naturally synthesized by microorganisms (Hsueh et al. 2017). It possesses exceptional biochemical characteristics, including water absorption, moisture retention, and biocompatibility. As a novel, environmentally friendly biomaterial (Ashiuchi 2002), it has extensive applications across various fields, including food, cosmetics, agriculture, medicine, and environmental fields (Hu et al. 2023). Therefore, γ-PGA biosynthesis has garnered significant attention. γ-PGA-producing strains can be categorized into two groups: glutamic acid-dependent and glutamic acid-independent. The former requires an external supply of glutamate to generate γ-PGA, whereas the latter can produce γ-PGA without additional glutamate supplementation (Jose et al. 2018). Notably, glutamic acid-dependent strains exhibit higher γ-PGA production than their glutamic acid-independent strains, making them the primary choice for industrial γ-PGA production (Jose et al. 2018).

The microbial γ-PGA synthesis pathway comprises three primary stages: precursor synthesis, polymerization transfer, and catabolism. Key metabolic pathways, such as glycolysis (EMP), pentose phosphate pathway (PPP), tricarboxylic acid (TCA) cycle, and amino acid metabolism, play essential roles in γ-PGA biosynthesis (Li et al. 2022). L- glutamate, as a precursor, can be converted into D-glutamate through multiple enzymatic routes (Ko et al. 1998). These L-glutamate and D-glutamate molecules undergo polymerization facilitated by the PgsBCA multi-protein complex to produce γ-PGA, which is subsequently secreted from the cell (Ashiuchi et al. 2001a; Ashiuchi et al. 2001b). This polymerization process requires ATP consumption. The polyglutamic acid synthase (Pgs) is encoded by the *pgs* operon and encompasses four genes: *pgsB, pgsC, pgsA*, and *pgsE* (Shih and Van 2001). In addition, the gene encoding γ-PGA hydrolase (PgdS) is located downstream of the *pgs* operon. Specifically, PgsB is an ATP-dependent amino ligase that catalyzes γ-PGA formation (Kimura et al. 2009; Tomosho et al. 2008). PgsC is a cell membrane component within the γ-PGA synthesis system, featuring

structural resemblance to the N-acetyltransferase domain of N-acetylglutamic acid synthase (Yamanaka et al. 2008). PgsA includes a cell membrane-anchoring region (Ashiuchi 2002) that may have implications for γ-PGA synthesis or transport (Nordlund and Eklund 1995; Rusnak and Mertz 2000).

The regulatory mechanisms governing γ-PGA biosynthesis remain incompletely understood, with limited research in this area. Zeng et al. compared the genomic differences between glutamate-dependent and glutamate-independent strains, indicating 13 genes related to γ-PGA biosynthesis are mutated in glutamate-dependent strains. However, the relationship between these mutations and glutamate dependence has not yet been conclusively established (Zeng et al. 2017). Sha et al. explored the dependence mechanism of *Bacillus subtilis* NX-2 on glutamic acid during γ-PGA production through transcriptome analysis. Their findings revealed that the addition of glutamate significantly up-regulated genes associated with glycolysis, PPP, TCA cycle, glutamic acid synthesis, and γ-PGA synthesis. Overexpression of these genes caused the accumulation of γ-PGA, demonstrating the pivotal role of intracellular glutamic acid synthesis in regulating γ-PGA production in glutamate-dependent strains (Sha et al. 2000). Li et al. preliminarily investigated the co-production mechanism of γ-PGA and nattokinase by transcriptome technology. Their study revealed the up-regulation of gene expression related to carbohydrate metabolism. Furthermore, by analyzing major metabolic pathways, such as carbohydrate metabolism, potential target genes for enhancing γ-PGA production were observed (Li et al. 2021).

Previous studies have shown that γ-PGA biosynthesis is regulated by two intracellular signal transduction mechanisms. ComA is a DNA-binding transcription factor and is the corresponding regulator of the two-component ComP-ComA system. At high cell densities, the cell density signal of ComX is transferred from phosphorylated ComP to phosphorylated ComA. This event induces the expression of DegQ, which transfers the cell density signal to the DegS-DegU binary system. This can promote DegU phosphorylation, and the combination of phosphorylated DegU to the pgsBCA gene promoter activates its expression (Msadek et al. 1991; Dubnau et al. 1993; Tran et al. 2000). Phosphorylated DegU directly engages the pgsBCA promoter, thereby activating gene expression. Consequently, knockout of DegU and SwrA results in the loss of γ-PGA synthesis capability (Ohsawa et al. 2009; Stanley et al. 2005). SwrA and DegU facilitate the expression of the *pgsBCA* operon through protein-protein interactions, serving as key factors in activating its expression. However, the relationship between these regulatory factors and the addition of glutamate remains unclear (Ogura and Tsukahara 2012).

To elucidate the regulatory mechanisms governing γ-PGA biosynthesis, this study focused on the glutamate-dependent strain, *B. subtilis* SCP017-03. The effects of exogenous glutamate supplementation on γ-PGA production and cell growth were investigated. Moreover, a comparison and analysis of the differential expression of bacteria at the protein and transcription levels in the presence and absence of glutamate were conducted using transcriptome and proteomics technologies. This analysis focused on the differential expression observed in glycolysis, tricarboxylic acid cycle, pentose phosphate pathway, glutamic acid metabolism, and γ-PGA synthesis pathway resulting from the addition of glutamate. Based on these findings, fermentation conditions were optimized, with a significant improvement in the yield of γ-PGA. This study can provide a profound and systematic understanding of the molecular mechanisms

underlying glutamate dependence in various γ-PGA strains. Furthermore, this study can offer a valuable theoretical foundation for future gene modification endeavors aimed at achieving high-yield γ-PGA production.

Materials and Methods

Strain and media

Bacillus subtilis SCP017-03 (CGMCC 60083) was isolated and preserved in our laboratory. A single colony of SCP017-03 was cultivated in LB liquid medium and cultured overnight at 37℃. The resulting

culture was subsequently transferred to a triangular flask containing a fermentation medium with the following composition: glucose 60.0 g/L, yeast powder 12.0 g/L, sodium glutamate 50.0 g/L, KH_2PO_4 0.5 g/L, K_2HPO_4 0.5 g/L, and $MgSO_4$ 0.1 g/L. The initial fermentation conditions were as follows: initial pH of 7.0, culture temperature of 37℃, agitation at 220 rpm, culture medium containing 10% liquid content, inoculation amount of 4%, and fermentation period of 72 h.

Determination of related indexes in fermentation process

Glutamate content in the fermentation broth was quantified using an enzyme-based method employing a biosensor (SBA-40c, Shan-Dong Academy of Sciences, China). Determination of the total sugar content in the fermentation broth involved diluting the broth to appropriate concentrations and employing the sulfuric acid-acetone method (Cuesta et al. 2003). The purification and concentration determination of γ-PGA referred to the method proposed by Chang (Chang et al. 2022). The steps comprised 5 mL of the fermentation broth, adjusted to pH 3 with 50% trichloroacetic acid, centrifugation at 10,000 rpm for 10 min to eliminate bacteria, collection of the supernatant, restoration of the pH to 7, addition of fourfold anhydrous ethanol, and precipitation overnight at 4℃. The precipitate was collected by centrifugation at 10000 r/min, and the 10,000 rpm, resulting in a crude γ-PGA product that was further obtained by freeze-drying. Subsequently, the crude γ-PGA product was dissolved in 5 mL of ddH_2O, and its absorbance at 400 nm was measured using the CTAB method. Finally, the molecular weight of γ-PGA was determined by SDS-PAGE (Yamaguchi et al. 1996).

Transcriptome analysis

Fresh seed liquid of strain SCP017-03 was inoculated into two fermentation media: one without glutamate and the other with glutamate. Cultures were maintained at 37℃ and agitated at 220 rpm. After 20 h of fermentation, bacterial cells were collected by centrifugation and subsequently sent to Beijing Nuohe Zhiyuan Technology Co., Ltd. for Qualcomm RNA sequencing (RNA-Seq). A cDNA library was successfully constructed and sequenced using the Illumina NovaSeq 6000 high-throughput sequencing platform. The sequence data was deposited to the NCBI Sequence Read Archive (SRA,

https://www.ncbi.nlm.nih.gov/sra) with the accession number PRJNA 1057989. Quality control and data filtering were performed using FastQC software (Version 0.11.5). Low-quality RNA-Seq reads (reads with Qpred ≤ 20, representing more than 50% of the total reads) were removed, and the filtered reads were subjected to genome mapping analysis using Bowtie 2 software (Langmead and Salzberg 2012) against the *B. subtilis* subsp. natto Best 195 for genome mapping analysis. The transcript assembly and quantification were performed using featureCounts in the subread software. The relative quantitative value of transcripts was measured using fragments per kilobase of transcript per million mapped reads (FPKM), with transcripts having an FPKM value ≥ 1 considered effectively expressed. From the RNA-seq results, certain genes related to γ-PGA synthesis were selected for validation using qRT-PCR. The 16S rRNA internal reference gene served as the normalization standard, and the specific primers used are listed in Table S1. Three replicates were performed for each sample.

Proteomic analysis

The fermentation broth collected at the 6th and 20th hour underwent centrifugation and was subsequently sent to Beijing Nuohe Zhiyuan Technology Co., Ltd. for further processing. Data are available via ProteomeXchange with identifier PXD049242. This process included protein quality assessment, enzyme digestion, desalting, iTRAQ labeling, chromatographic separation, and mass spectrometry analysis. The mass spectrometry data were matched against the *B. subtilis168* protein database from NCBI, and the retrieval results were filtered using MaxQuant software. This filtering process selected spectral peptides with a reliability exceeding 99%, while peptides and proteins with an FDR exceeding 0.01 were eliminated. Proteins showing up-regulated expression were identified when FC > 2.0, and PALUE < 0.05. Conversely, down-regulated proteins were identified when FC < 0.50 and PALUE < 0.05.

Results

Effects of glutamate addition on cell growth and γ-PGA synthesis

To assess the effect of glutamate addition on fermentation, *B. subtilis* SCP017-03 was cultured under two conditions: one with glutamate addition (experimental group: GA) and another without glutamate addition (control group: CK). The differences in glucose and glutamate consumption, cell growth, and γ-PGA yields were compared. As depicted in Fig. 1a, the results revealed no significant differences in cell growth or carbon source consumption between both groups during the initial 0–4 h of fermentation. However, after 10 h, cell growth in the GA group lagged significantly behind that in the CK group. Between 18 and 48 h of fermentation, the differences in cell growth and glucose consumption between the experimental and control groups were more pronounced. At the 36-hour point, the OD_{600} value difference between the two groups reached the maximum, with CK in the control group at 6.4, while GA in the experimental group measured 4.8. After 12 h, glucose consumption in the GA group slowed, with the glucose content stabilizing at 25 g/L after 72-hour fermentation. However, the control group exhibited

faster sugar consumption, exhausting the glucose supply after 60th hour of fermentation. Sugar consumption correlated precisely with differences in cell growth. Furthermore, the GA group initiated γ-PGA synthesis after 8 h of fermentation and continued to accumulate. After 18 h, the γ-PGA content reached 16.7 g/L, peaking at 36.5 g/L after 48 h of fermentation, remaining relatively stable until the end of fermentation. The residual concentration of glutamate in the fermentation broth of the GA group gradually decreased from 50 g/L to 35 g/L after 60 h of fermentation, indicating a modest reduction of 15 g/L over the course of fermentation. This observation suggested that the bacterial cells of this strain synthesized a certain amount of glutamate.

The γ-PGA generated in the fermentation broth was assessed using SDS-PAGE (Fig. 1b). The figure illustrates that the molecular weight of γ-PGA produced by this strain significantly exceeded 200 kD. However, as fermentation progressed, there was a slight reduction in molecular weight.

Transcriptome analysis of strain scp017-03 in response to glutamate addition

The RNA samples from each group were subjected to sequencing using an Illumina NovaSeq 6000 high-throughput sequencing platform. The sequencing output data exhibited base quality values of Q30 and Q20 exceeding 95% and 98%, respectively, with a sample sequencing error rate of less than 0.03%. These metrics complied with stringent quality standards for Illumina sequencing. Table 1 shows the alignment results for each sample against the reference genome. All six samples achieved a total mapping rate, were successfully aligned to the genome via sequence mapping, and each exhibited unique alignment positions on the reference sequence.

Table 1
Mapping results of strain SCP017-0 transcriptome

Sample.name	CK1	CK2	CK3	GA1	GA2	GA3
Total reads	8754356	7523564	7800772	7724204	7734902	7438034
Total mapped reads	8621421	7418727	7684771	7636601	7638796	7325040
Uniquely mapped reads	8425126	7275289	7526589	7500556	7495239	7168957
Multiple mapped reads	196295	143438	158182	136045	143557	156083
Total mapping rate	98.48%	98.61%	98.51%	98.87%	98.76%	98.48%
Uniquely mapping rate	96.24%	96.7%	96.49%	97.1%	96.9%	96.38%
Multiple mapping rate	2.24%	1.91%	2.03%	1.76%	1.86%	2.1%

Statistical analysis of differentially expressed genes was conducted using the following screening criteria: log2 (FoldChange) > 0 or padj < 0.05. A total of 1867 differentially expressed genes were identified, comprising 862 up-regulated and 1005 down-regulated genes. Subsequently, ClusterProfiler

software was utilized to perform GO function enrichment analysis and KEGG pathway enrichment analysis on the sets of differential genes, with a significance threshold set at padj < 0.05. GO function enrichment analysis indicated the presence of both up-regulated and down-regulated genes within three categories: biological process (BP), cellular component (CC), and molecular function (MF) (Fig. 2). These findings suggested that the addition of exogenous glutamic acid significantly affected various metabolic pathways in this strain. Furthermore, the enrichment results of the KEGG pathway analysis encompassed the differentially expressed genes and certain genes related to γ-PGA synthesis (Fig. 3).

The phosphotransferase system (PTS) is the primary mechanism employed by bacteria to uptake hexose, hexitol, disaccharides, and other carbohydrates. As shown in Fig. 3, the addition of exogenous glutamate led to the differential expression of *ybbF* and *sacX* genes within the sucrose metabolism system (EIIBCA or EIIBC component). Their $\log_2$FC values were − 2.03 and + 2.65, respectively. The carbohydrates transported into the membrane entered not only the central metabolic pathway but also the polysaccharide synthesis (EPS). Within the EMP pathway consisting of energy consumption and productivity stages, gene expression in the energy consumption stage, including *pgi* (glucose-6-phosphate isomerase), *glpX* (fructose 1,6-diphosphatase), and *pfkA* (ATP-dependent phosphofructokinase), was slightly down-regulated. Conversely, during the production stage of Pyr synthesis from G-3-P, the expression of these five genes was significantly up-regulated. These genes include *fbaA* (fructose-diphosphate aldolase), *pgm* (glycerophosphate mutase), *eno* (enolase), *gapA*, and *gapB* (glyceraldehyde-3-phosphate dehydrogenase). Consequently, the addition of exogenous glutamate enhanced the EMP pathway. In the PPP pathway, the expression of *zwf* (glucose-6-phosphate dehydrogenase) and *ykgB* (glucose-6-phosphate esterase) was down-regulated by factors of 1.07 and 2.03, respectively, while *ganZ* (6-glucose-6-phosphate dehydrogenase) witnessed an up-regulation in expression.

The TCA cycle is initiated by the condensation of acetyl-CoA and oxaloacetic acid to produce citric acid. Acetyl-CoA is formed through the oxidative decarboxylation of pyruvate under aerobic conditions. Figure 4 illustrates that most genes within the TCA cycle pathway were down-regulated in the GA group. Notably, the $\log_2$FC values for *citZ* and *icd* were − 1.76 and − 0.72, respectively, with only the *sdhABC* gene (encoding succinate dehydrogenase) displaying up-regulation. In addition, the coding genes responsible for the pyruvate dehydrogenase complex, which catalyzed the decarboxylation of pyruvate to synthesize acetyl coenzyme A, were down-regulated. For example, the *acoC* gene (encoding dihydrooctylamide transacetylase) exhibited a down-regulation of 4.69 times, while the *idh* gene (encoding lactate dehydrogenase), responsible for transforming pyruvate into lactic acid, displayed an up-regulation of 2.74 times. These findings suggested that the synthesis of high-viscosity γ-PGA by cells resulted in reduced dissolved oxygen levels in the culture solution, thereby reducing the flow of substances into the tricarboxylic acid pathway.

L-glutamic acid was converted into D-glutamic acid through the action of RacE (glutamate racemase), and these compounds were subsequently utilized in the synthesis of γ-PGA by γ-PGA synthetase. Figure 3 demonstrates an up-regulation in the expression of the *glnA* gene (encoding glutamine synthetase) and

racE, with $\log_2$FC values of 0.86 and 1.77, respectively. This upregulation enhanced the production of the precursor D-glutamic acid for γ-PGA, thereby strengthening γ-PGA synthesis. Notably, the *pgsBCA* gene cluster (encoding γ-PGA synthetase) was significantly up-regulated, with $\log_2$FC values of 2.63, 2.83, and 2.78, respectively. The *pgsBCA* operon was regulated by DegS-DegU and ComA-ComP two-component systems. In the CK group without γ-PGA synthesis, the FPKM value of the *degU* gene was 2396, and the FPKM values of the *pgsBCA* gene cluster were 859, 744, and 1243, indicating baseline expression of the γ-PGA synthesis system in the absence of exogenous glutamate. However, the *pgsBCA* operon was further activated upon addition of exogenous glutamate, with the FPKM value of the *pgsA* gene reaching 8533. These two-component systems can interact with phosphorylated ComA to induce degQ expression. Nevertheless, the expression levels of *comA, comX, comQ*, and *degQ* genes in this strain remained low. For example, the FPKM value of *degQ* in the GA group was only 69. After γ-PGA synthesis, the cells required the action of γ-PGA hydrolase to release γ-PGA. This process may involve three genes, *pgdS, cwlO*, and *ggt*. Transcriptome analysis revealed that these three genes exhibited low expression in the GA group, with FPKM values of 27, 282, and 266, respectively. Furthermore, the expression of *ggt* in the CK group was significantly higher than that in the GA group.

qPCR analysis of genes related to γ-PGA biosynthesis

Selected genes related to γ-PGA biosynthesis were subjected to qPCR analysis to validate the findings of transcriptome analysis. To investigate dynamic changes in key genes and regulatory factors during fermentation, samples were collected for qPCR analysis at three time points: 10 h (immediately following γ-PGA synthesis initiation), 20 h, and 48 h (when γ-PGA accumulation peaked). The results are presented in Table 2. After 10-hour fermentation, most genes in the TCA cycle, PPP pathway, and glutamic acid synthesis pathway exhibited slight down-regulation, except for a few genes such as *citA*, *gltP*, and *rocA*. In the γ-PGA synthesis module, only the expression of the regulator DegQ showed a 0.67-fold decrease, and the genes encoding γ-PGA synthetase were significantly up-regulated. Specifically, *pgsB* expression increased by 4.94 times, and *pgsA* expression increased by 4.63 times. Moreover, the genes *pgdS* and *cwlO*, associated with γ-PGA hydrolysis, were up-regulated, with fold changes of 2.73 and 1.47, respectively. At the 20-hour point, genes in the central metabolic pathway generally showed down-regulation, except for the *eno* gene in the EMP pathway and the *sdhA* gene in the TCA cycle, consistent with the transcriptome analysis results. Notably, *pgdS* exhibited slight downregulation. In addition, the γ-PGA synthesis module consistently displayed up-regulated expression. In the late stage of fermentation (48 h), owing to significant nutrient depletion in the culture medium, gene expression in the central pathway decreased. Concurrently, as γ-PGA accumulation peaked, some γ-PGA was hydrolyzed by bacterial cells to maintain its state, as evidenced by the substantial upregulation of *cwlO* gene expression, with a fold change of 21.93. Throughout the fermentation process, the regulatory factor degQ was consistently down-regulated, whereas *degS* and *degU* were up-regulated, indicating complex interactions within the DegS-DegU two-component system.

Table 2
Comparison of expression of key genes in γ-PGA synthesis by qPCR of strain *SCP017-03* grown with glutamate and without glutamate at different fermentation times

Gene	10h	20h	48h
pfkA	4.30	0.60	2.18
pgi	2.93	0.75	1.63
eno	6.30	2.97	2.18
pdhA	2.52	0.05	0.11
citB	1.87	1.99	0.54
icd	1.50	0.40	0.53
fumC	2.69	0.44	0.43
ykgB	1.06	0.23	0.22
zwf	1.97	0.88	3.34
ganZ	2.80	0.47	0.20
gltP	0.67	0.16	0.04
rocA	0.20	2.86	5.96
racE	4.42	0.35	0.01
degQ	0.67	0.32	0.05
degU	1.36	1.02	1.41
degS	7.59	2.03	1.13
pgsA	4.63	2.45	18.83
pgsB	4.94	4.82	21.26
pgsC	3.23	9.38	12.21
glnA	0.92	1.64	0.94
putM	1.55	0.03	0.06
pgdS	2.73	0.76	1.71
comA	2.45	0.58	6.70
cwlO	1.47	4.89	21.93

Notes: The numbers in the table represent gene expression levels, which have been normalized to the 16S rRNA internal reference gene.

Proteomic analysis of strain SCP017-03 in response to glutamic acid addition

Strain SCP017-03 was subjected to fermentation in culture media with or without exogenous glutamate (GA group). Cell samples were collected at 6 and 20 h after fermentation. Protein analysis was conducted using 4D-label-free technology, leading to the identification of 2,161 proteins and 13,243 peptides. Each sample (CK6h, GA6h, CK20h, and GA20h) was then quantified. Differentially expressed proteins were identified based on criteria where the FC > 2.0 or < 0.5 and Pvalue < 0.05, with a significance level of $P < 0.05$. After 6 h of fermentation, a comparison between the GA and CK groups (Fig. 4a) revealed 328 differentially expressed proteins. These included 162 up-regulated and 166 down-regulated proteins. After 20 h of fermentation (Fig. 4b), 279 differentially expressed proteins were identified, comprising 142 up-regulated upregulated and 137 down-regulated proteins. A comparison within the GA group, specifically between 20 and 6 h of fermentation (Fig. 4c), yielded 297 differentially expressed proteins. Among them, 158 were up-regulated and 139 were down-regulated. Similarly, 296 differentially expressed proteins were observed in the CK group (Fig. 4d), with 162 up-regulated and 136 down-regulated proteins. The volcano plot of the differential proteins visually illustrated that the majority of proteins (represented in black) exhibited no significant differences. Proteins with differences in expression are denoted in red (up-regulated) and green(down-regulated) (Fig. 4).

The enrichment category of differential proteins GO in the GA group exhibited significant changes between the 6-hour and 20-hour fermentation periods, whereas the corresponding changes in the CK group were relatively minor (Fig. 5a and 5b). Compared to differentially expressed proteins associated with BP in the CK group, those in the GA group at 6 h of fermentation were primarily involved in processes related to localization (25 proteins), transportation (21 proteins), and coenzyme biosynthesis (6 proteins). Furthermore, differentially expressed proteins linked to “cell composition (CC)” were predominantly associated with specific cellular structures. As the fermentation duration reached 20 h, the BP processes in the GA group emphasized transmembrane transport (13 proteins), transport (23 proteins), and localization (24 proteins), while the CC processes centered on membrane-related components (28 proteins) and the ABC transport complex (2 proteins). In the MF category, the focus shifted towards hydrolase activity (four proteins). Similarly, the analysis of GO enrichment for differential proteins in both the GA and CK groups (Fig. 5c and 5d) revealed that the differentially expressed proteins in the GA group were primarily concentrated in the BP (22 localized proteins) and CC (30 membrane-related proteins) categories, whereas in the CK group, the emphasis was mainly on the CC (28 membrane-related proteins) and MF (38 proteins associated with hydrolase activities) categories.

Table 2 illustrates that after 6 h of fermentation, the protein expression within the central metabolic pathways of the GA group exhibited slight changes compared to the CK group. For example, in the EMP pathway, with the exception of GlpX (fructose 1,6-diphosphatase), which showed a modest 0.31-fold up-regulation, other proteins displayed down-regulated expression. Notably, Pgi, Fbp, and Eno had log2FC values of -0.58, -0.93, and − 0.82, respectively. In the TCA cycle, only PdhB (β subunit of pyruvate dehydrogenase E1 component) and PDHC (α subunit of DNA polymerase III) exhibited slight increases in

protein expression, with log_2FC values of 0.47 and 0.59, respectively. Conversely, the expression of other proteins, including SdhA (protein subunit of succinate dehydrogenase), notably decreased, with a log_2FC value of -1.25. Changes in protein expression within the PPP pathway were relatively minimal. After 20-hour fermentation, the log2FC values for certain proteins in these metabolic pathways underwent substantial changes, with most proteins in the EMP pathway showing increased expression. In the TCA cycle, aside from PdhABC, which was up-regulated by 0.71, 1.38, and 1.16, the expression of other proteins aligned with the transcriptome results, indicating down-regulation. Similarly, the expression of PPP pathway proteins was consistent with the results of the transcriptome analysis. Furthermore, this study analyzed protein expression at different stages of fermentation (20 and 6 h) for different treatments. The results revealed that in the GA group, protein expression in the EMP pathway was predominantly up-regulated, whereas the CK group exhibited the opposite trend. However, enzyme expression in the TCA cycle and PPP pathway remained largely consistent between the two groups, with PPP pathway enzymes being down-regulated.

After a 6-hour fermentation period, a comparison between the GA and CK groups revealed notable changes in the expression of proteins involved in the glutamate synthesis pathway (Table 2). Specifically, the expressions of RacE and RocG in the glutamate synthesis pathway were up-regulated in the GA group, with log_2FC values of 1.78 and 0.15, respectively. In contrast, the expression of other proteins within this pathway decreased, with GltB (glutamate synthase domain 3) showing the most significant down-regulation, marked by a log_2FC value of -3.28. However, proteins and regulatory factors related to γ-PGA synthesis exhibited only slight changes, such as the log_2FC values of -0.39 for DegQ, -0.78, DegU, and − 0.19 for PgsA. However, after a 20-hour fermentation period, substantial changes were observed in the expression of histones in both the GA and CK groups. In the glutamic acid synthesis pathway, the log_2FC value of PurQ increased from − 0.29 to 1.89, while RacE exhibited an increase in log_2FC from 1.76 to 4.12. Concurrently, the expression of other proteins in this pathway was also down-regulated. Within the γ-PGA synthesis system, both PgsA and PgsB were up-regulated, with log_2FC values of 1.68 and 3.05, respectively. Notably, the protein expression of DegQ and DegS in the DegS-DegU two-component system diverged from the transcriptome analysis. Specifically, the log_2FC values for regulatory factors DegQ and DegS were 1.9 and − 0.44, respectively. However, the protein expression of the ComP-ComA system aligned with aforementioned transcriptional analysis, with the ComA regulatory factor exhibiting down-regulation. Additionally, there was a general increase in enzymatic activity within the glutamate synthesis pathway. For example, the activity of glutamate racemase (RacE), which was responsible for the transformation of D-glutamic acid and L-glutamic acid, increased by 4.12 times, while the expression of γ-PGA hydrolase (Pgds) decreased by 2.24 times.

Table 2 presents a significant increase in γ-PGA polymerase activity within the GA group after 20 h compared to the 6-hour mark. Notably, the log_2FC values for PgsA and PgsB were 2.04 and 3.83, respectively. Furthermore, it was observed that γ-PGA synthetase activity in the CK group after 20 h of fermentation was lower than that at the 6-hour mark. γ-PGA synthetase activity notably increased by a factor of 2.05. This observation suggested that the expression of the γ-PGA synthetase gene exogenous

glutamic acid. However, the translation of this mRNA into protein may have been influenced by other genes or regulatory factors, resulting in the reduced activity of γ-PGA synthetase.

Optimization of fermentation conditions

Preliminary optimizations were conducted for carbon and nitrogen sources in an effort to enhance γ-PGA yield during fermentation. The results of carbon source optimization are presented in Fig. 6a. Among the tested options, glucose as the carbon source yielded the highest γ-PGA production at 38.35 g/L, followed by sucrose (36.5 g/L), starch (33.9 g/L), and xylose (32.6 g/L). Conversely, when glycerol was employed as the carbon source, the γ-PGA yield was the lowest at 22.8 g/L. Figure 6b illustrates that yeast powder was a superior nitrogen source, yielding a γ-PGA production of 40.12 g/L. Other nitrogen sources, including pancreatic peptone, soybean peptone, and bean cake powder, yielded approximately 37.5 g/L γ-PGA. In contrast, beef paste and corn steep liquor, when applied as nitrogen sources, resulted in lower yields of 14.32 g/L and 16.2 g/L, respectively. Consequently, the optimal carbon source was glucose, and the preferred nitrogen source was yeast powder.

The results revealed that during the synthesis of γ-PGA, the transcriptional activity of related genes, including those associated with glycolysis, tricarboxylic acid cycle, and PPP pathway, decreased. This decrease could be related to the increased fermentation broth viscosity and the impact of dissolved oxygen. To optimize fermentation, four organic carriers (w/v: 0.5%) were selected. The organic carriers included n-hexane, n-heptane, n-dodecane, and n-hexadecane. Figure 7a illustrates that when n-hexadecane was introduced at the onset of fermentation, the highest γ-PGA yield was achieved, reaching 42.9 g/L. This was followed by n-hexane and n-heptane, with γ-PGA yields of 38.2 g/L and 36.2 g/L, respectively. In contrast, n-dodecane afforded the lowest γ-PGA yield, only reaching 9.24 g/L. Considering the potential impact of organic matter added at the early stages of fermentation on bacterial growth, the organic carrier was introduced into the fermentation for 24 h. Figure 7b shows that, with the addition of the organic carrier after 24-hour fermentation, the γ-PGA production increased by 9.4 g/L in the n-heptane group and by 17.06 g/L in the n-dodecane group. Among these, the n-heptane group achieved the highest γ-PGA output of 45.6 g/L. Notably, there was no significant difference observed between the n-hexadecane group and the n-hexane group, with respective outputs of 43.3 g/L and 35.9 g/L. Therefore, n-heptane was selected for liquid fermentation for 24 h.

Scale-up experiment of batch feeding in 5L fermentor

In the context of shaking flask conditions, the fermentation duration was insufficient, resulting in a low dissolved oxygen concentration and inadequate carbon source concentration in the later stages. These limitations restricted the successful synthesis of γ-PGA. Therefore, fermentation processes were optimized using a 5 L fermentor. The fermentation parameters were set to 500r/min for agitation, 2 L/min for aeration, and a pH of 7. Glucose was added when the total sugar content decreased below 50 g/L. Figure 8 illustrates the dynamic changes in various fermentation parameters. After 24 h of fermentation,

the cell growth (OD_{600}) reached 3.195, the total sugar residue was 24.09 g/L, and the γ-PGA yield reached 36.29 g/L. However, glutamate content in the fermentation broth remained relatively stable. At this point, an additional 100 g of glucose was introduced, increasing the total sugar content to 55.82 g/L. By the 32-hour point, the glutamate in the fermentation broth decreased to 33.72 g/L, indicating a consumption of 16.27 g/L. Bacterial cell growth increased to 7.68, prompting the second addition of 100 g glucose. At the 48-hour point, bacterial growth (OD_{600}) peaked at 10.82, while the total sugar residue reached 43.67 g/L. To sustain fermentation, 50 g of glucose was added. During the fermentation period from 54 to 96 h, as bacterial cells entered the decay phase and nutrient consumption decreased, the last feeding occurred at 54 h, with 50 g of glucose added. At 82 h of fermentation, the total glucose consumption reached 84.18 g/L, and γ-PGA production peaked at 92.5 g/L, subsequently stabilizing. Towards the end of fermentation, bacterial growth (OD_{600}) decreased to approximately 8.0, with total sugar and glutamate levels in the tank measuring 18.3 g/L and 31.6 g/L, respectively.

Discussion

Currently, industrial production of γ-PGA primarily relies on glutamate-dependent strains, necessitating the addition of exogenous sodium glutamate for γ-PGA synthesis. Therefore, thorough investigation of the mechanisms underlying glutamate dependence is crucial. However, research in this area has been limited. This study compared and analyzed differences in SCP017-03 gene expression at both the transcriptional and protein levels by employing transcriptomics and protein genomics. Different from the findings of Sha et al., where nearly all genes in the three central metabolic pathways were significantly up-regulated, the transcriptome results showed a significant down-regulation in the expression of coding genes in the PPP and TCA cycle pathways. Conversely, most of the coding genes in the EMP pathway were up-regulated. This disparity was attributed to the decreased dissolved oxygen in the culture medium caused by the highly viscous γ-PGA product. This decreased the expression of genes encoding the TCA and PPP pathways. However, most coding genes in the glycolytic pathway were up-regulated, promoting pyruvate accumulation and directing metabolism towards the fermentation product, lactic acid. The significant up-regulation of dehydrogenase-encoding genes upon glutamic acid addition further validated this hypothesis. Building upon this analysis, subsequent experiments in this study enhanced γ-PGA production by improving the dissolved oxygen levels in the culture medium. Interestingly, the *pgsBCA* gene cluster responsible for γ-PGA synthesis was present in the genome of the control group without exogenous glutamic acid, with FPKM values reaching 859, 744, and 1243, respectively, although γ-PGA synthesis did not occur. This suggested that the lack of sufficient glutamic acid as a precursor within the cells and protein-level regulation may be contributing factors. In contrast, the experimental group supplemented with exogenous glutamate exhibited significant up-regulation in the expression of the *pgsBCA* gene cluster, with $\log_2$FC values of 2.63, 2.83, and 2.78, respectively, which was consistent with the findings of Sha et al. (Sha et al. 2019a). In summary, the response mechanism to glutamate addition varied among different γ-PGA-producing strains, highlighting the complexity of this phenomenon.

The gene encoding the γ-PGA degrading enzyme *pgdS* was located downstream of the *pgsBACE* operon. The PgdS was secreted into the extracellular space, which facilitated γ-PGA degradation. Additionally, previous studies have shown γ-glutamyltranspeptidase (GGT) and DL-endopeptidase (CwlO) (Ashiuchi et al. 2006; Morelli et al. 2014; Mitsui et al. 2011). In this study, observations were conducted in both the control group (CK), lacking glutamate, and experimental group (GA), with glutamate supplementation. The *pgdS* exhibited minimal expression in both groups, whereas the expression of *cwlO* remained low, with FPKM values of 59 and 282, respectively. However, the expression level of *ggt* decreased, with its FPKM dropping from 1231 to 266. Feng et al. conducted individual knockout experiments of the *pgdS*, *ggt*, and *cwlO* genes in glutamate-independent strains. The γ-PGA yield improved only when the *cwlO* gene was singly knocked out, and further enhancements were observed through simultaneous knockout of the *pgdS* and *ggt* genes (Feng et al. 2014). Similarly, Scoffone et al. reported a doubling of γ-PGA yield after double knockout of *pgdS* and *ggt* in glutamate-dependent strains (Scoffone et al. 2013). Furthermore, overexpression of *pgdS* significantly increased γ-PGA production (Sha et al. 2019b).

The proteomic analysis in this study revealed that genes in the energy consumption stage of the glycolytic pathway exhibited a slight down-regulation, whereas genes associated with the energy production stage were up-regulated. Furthermore, the PPP and TCA cycle pathways displayed noticeable down-regulation, aligning perfectly with the metabolic pathway responses observed in transcriptome sequencing following glutamate supplementation. Additionally, dynamic changes in the expression of key genes involved in γ-PGA synthesis were analyzed by qPCR at various fermentation time points. The results indicated that during the initial stage of fermentation (10 h), the genes from all central metabolic and γ-PGA synthesis pathways were up-regulated. As fermentation progressed (20 h and 48 h), the genes associated with γ-PGA synthesis continued to display up-regulation, while those related to central metabolic pathways exhibited a declining trend. In summary, for glutamic acid-dependent bacteria, the addition of glutamate had a dual purpose: activating γ-PGA synthetase expression and providing the ample supply of glutamate necessary for γ-PGA synthesis.

The mechanism underlying the high yield of γ-PGA is complicated and encompasses aspects such as glutamate supply, γ-PGA synthesis, transport, secretion, energy metabolism, and glutamate metabolism. In this study, the qPCR analysis revealed that in the experimental group supplemented with glutamate, the expression of the *pgsBCA* gene cluster exhibited significant up-regulation throughout the 10th to 48th hours of fermentation, compared to the control group. Moreover, the genes *degS* and *degU* displayed substantial up-regulation at the 10th and 20th hours of fermentation, with a slight increase at the 48th hour, while *degQ* showed down-regulation. Transcriptome analysis indicated that the coding genes *comX*, *comA*, and *swrA* were expressed at low levels during the 20th hour of fermentation and were slightly down-regulated after glutamate addition. In parallel, proteomic analysis demonstrated a significant up-regulation of *comP* expression at the sixth hour of fermentation. Moreover, the quorum sensing system (QS system), which was known to influence γ-PGA synthesis by primarily affecting *comA* expression and indirectly regulating γ-PGA synthesis, has been considered (Omer et al. 2015; Hu et al. 2022). The study findings indicated significant down-regulation of the coding genes for Spo0K permease (*oppABCDF*) and

phosphatase RapC (*rapHCFK*), while the expression of *comA* was slightly down-regulated. This suggested that *comA* may be regulated by other regulatory factors or genes.

Based on the comprehensive analysis of strain SCP017-03 at the physiological, protein, and transcription levels, along with the optimization of fermentation medium composition and enhanced dissolved oxygen conditions, several key findings emerged. Glucose and yeast extract were identified as the optimal carbon and nitrogen sources, respectively, increasing the yield of γ-PGA from 36.5 g/L to 40.12 g/L. However, the accumulation of the high-viscosity substance γ-PGA within the fermentation broth led to reduced aeration and inadequate dissolved oxygen levels, negatively affecting both cell growth and γ-PGA production. Researchers have proposed various strategies to address this challenge. For instance, Su et al. integrated the *vgb* gene (encoding hemoglobin) into the genome of a γ-PGA-producing strain (Su et al. 2010) to augment dissolved oxygen levels. Xu et al. successfully elevated γ-PGA yield to 39.4 g/L by introducing four different organic oxygen carriers into the fermentation medium (Zhang et al. 2012). Feng et al. proposed an aerobic plant cellulose experimental bed to enhance γ-PGA production (Feng et al. 2016). In this study, we focused on promptly mitigating dissolved oxygen deficiency in fermentation cultures and enhancing γ-PGA yield through the optimization of oxygen carriers. The results demonstrated a significant increase in γ-PGA production by introducing n-heptane during a 24-hour fermentation period, elevating the yield from 40.12 g/L to 44.3 g/L. Furthermore, in a 5 L fermentor, the yield reached an impressive 95.2 g/L after batch feeding with sucrose.

In summary, this study presented a pioneering integration of transcriptome and proteome analyses, revealing the glutamate-dependent mechanism underlying γ-PGA synthesis in *B. subtilis*. Through a comparative analysis of strains cultured with and without glutamate, key genes involved in glycolysis, PPP, TCA cycle, and γ-PGA synthesis pathway were identified. This exploration revealed potential factors and metabolic pathways crucial to γ-PGA production, thereby providing an initial framework for understanding the production mechanism of γ-PGA. Subsequent research focused on fermentation optimization, resulting in a remarkable output of 95.2 g/L with the introduction of an oxygen carrier, demonstrating promising prospects for industrial-scale production. The findings of this study offer a valuable metabolic target for further enhancement of γ-PGA yield, with substantial significance for the large-scale production of targeted metabolites.

Declarations

Author contributions

Caiyun Wu, Fanglan Ge and Wei Li conceived and designed research. Caiyun Wu conducted experiments. Jiao Li, Yao Ren, Yutao Gou and Shuai Jing checked the data. Caiyun Wu wrote the manuscript. All authors read and approved the manuscript.

Funding

This study was funded by Sichuan Province Science and Technology Support Program (2022NSFSC1720), and Chengdu Science and Technology Program (2022-YF05-00631-SN).

Availability of data and materials

The data generated or analyzed during this study are included in this published article and its Additional file.

Declarations of Competing interests

The authors declare no competing interests.

References

1. Ashiuchi M, Kamei T, Baek DH, Shin SY, Sung MH, Soda K, Yagi T, Misono H (2001a) Isolation of *Bacillus subtilis*, a poly-γ-glutamate producer with high genetic competence. Appl Microbiol Biotechnol 57(5–6):764–769. https://doi:10.1007/s00253-001-0848-9
2. Ashiuchi M, Nawa C, Kamei T, Song JJ, Hong SP, Sung MH, Soda K, Misono H (2001b) Physiological and biochemical characteristics of poly-γ-glutamate synthetase complex of *Bacillus subtilis*. Eur J Biochem 268(20):5321–5328. i>https://doi:10.1046/j.0014-2956.2001.02475.x
3. Ashiuchi M (2002) Poly-γ-glutamic acid. Biopolymers 7:123–174. https://doi:10.1002/3527600035.bpol7006
4. Ashiuchi M, Shimanouchi K, Horiuchi T, Kamei T, Misono H (2006) Genetically engineered poly-gamma-glutamate producer from *Bacillus subtilis* ISW1214. Biosci Biotechnol Biochem 70(7):1794–1797. https://doi.org/10.1271/bbb.60082
5. Chang F, Li W, Hu H, Ge F, Chen G, Ren Y (2022) Chemical pretreatment and saccharification of corncob for poly-γ-glutamic acid production by *Bacillus subtilis* scp010-1. Process Saf Environ Prot 159:1184–1193. https://doi:10.1016/j.psep.2022.01.071
6. Cuesta G, Suarez N, Bessio MI, Ferreira F, Massaldi H (2003) Quantitative determination of pneumococcal capsular polysaccharide serotype 14 using a modification of phenol-sulfuric acid method. J Microbiol 52(1):69–73. https://doi:10.1016/s0167-7012(02)00151-3
7. Feng J, Gao W, Gu Y, Zhang W, Cao M, Song C, Zhang P, Sun M, Yang C, Wang S (2014) Functions of poly-gamma-glutamic acid (γ-PGA) degradation genes in γ-PGA synthesis and cell morphology maintenance. Appl Microbiol Biotechnol 98(14):6397–6407. https://doi:10.1007/s00253-014-5729-0
8. Feng X, Tang B, Jiang Y, Xu Z, Lei P, Liang J, Xu H (2016) Efficient production of poly–glutamic acid from cane molasses by *Bacillus subtilis* nx-2 immobilized on chemically modified sugarcane bagasse. J Chem Technol Biotechnol 91:2085–2093. https://doi:10.1002/jctb.4805
9. Hsueh YH, Huang KY, Kunene SC, Lee TY (2017) Poly-γ-glutamic acid synthesis, gene regulation, phylogenetic relationships, and role in fermentation. Int J Mo Sci 18(12):2644. https://doi:10.3390/ijms18122644

10. Hu LX, Zhao M, Hu WS, Zhou MJ, Huang JB, Huang XL, Gao XL, Luo YN, Li C, Liu K, Xue ZL, LiuY (2022) Poly-γ-glutamic acid production by engineering a DegU quorum-sensing circuit in *Bacillus subtilis*. ACS Synth Biol 11(12):4156–4170. https://doi:10.1021/acssynbio.2c00464
11. Hu H, Wu CY, Ge FL, Ren Y, Li W, Li J (2023) Poly-γ-glutamic acid-producing *Bacillus velezensis* fermentation can improve the feed properties of soybean meal. Food Biosci 53:102503. https://doi:10.1016/j.fbio.2023.102503
12. Jose AA, Sindhu R, Parameswaran B, Pandey A (2018) Production, characterization, and applications of microbial poly-γ-glutamic acid. Biosynth Technol Environ Chlg. https://doi:10.1007/978-981-10-7434-9_7
13. Ko YH, Gross RA (1998) Effects of glucose and glycerol on gamma-poly (glutamic acid) formation by *Bacillus licheniformis* ATCC 9945a. Biotechnol Bioeng 57(4):430–437. https://doi:10.1002/(sici)1097-0290(19980220)57:4<430::aid-bit6>3.0.co;2-n
14. Langmead B, Salzberg SL (2012) Fast gapped-read alignment with Bowtie 2. Nat Methods 9(4):357–359. https://doi:10.1038/nmeth.1923
15. Li D, Hou L, Gao Y, Tian Z, Fan B, Wang F, Li S (2022) Recent advances in microbial synthesis of poly-γ-glutamic acid: A Review. Foods 11(5):739. https://doi:10.3390/foods11050739
16. Li M, Zhang Z, Li S, Tian Z, Ma X (2021) Study on the mechanism of production of γ-PGA and nattokinase in *Bacillus subtilis* natto based on RNA-seq analysis. Microb Cell Factories 20(1):83. https://doi:10.1186/s12934-021-01570-x
17. Luo Z, Guo Y, Liu J, Qiu H, Zhao M, Zou W, Li S (2016) Microbial synthesis of poly-γ-glutamic acid: current progress, challenges, and future perspectives. Biotechnol Biofuels 9(134). https://doi:10.1186/s13068-016-0537-7
18. Mitsui N, Murasawa H, Sekiguchi J (2011) Disruption of the cell wall lytic enzyme CwlO affects the amount and molecular size of poly-γ-glutamic acid produced by *Bacillus subtilis* (natto). J Gen Appl Microbiol 57(1):35–43. https://doi:10.2323/jgam.57.35
19. Morelli CF, Calvio C, Biagiotti M, Speranza G (2014) pH-dependent hydrolase, glutaminase, transpeptidase and autotranspeptidase activities of *Bacillus subtilis* γ-glutamyltransferase. FEBS J 281(1):232–245. https://doi:10.1111/febs.12591
20. Msadek T, Kunst F, Klier A, Rapoport G (1991) DegS-DegU and ComP-ComA modulator-effector pairs control expression of the *Bacillus subtilis* pleiotropic regulatory gene degQ. J Bacteriol 173(7):2366–2377. https://doi:10.1128/jb.173.7.2366-2377.1991
21. Nordlund P, Eklund H (1995) Di-iron-carboxylate proteins. Curr Opin Struct Biol 5(6):758–766. https://doi:10.1016/0959-440x(95)80008-5
22. Ogura M, Tsukahara K (2012) SwrA regulates assembly of *Bacillus subtilis* DegU via its interaction with N-terminal domain of DegU. J Biochem 151(6):643–655. https://doi:10.1093/jb/mvs036
23. Ohsawa T, Tsukahara K, Ogura M (2009) *Bacillus subtilis* response regulator DegU is a direct activator of pgsB transcription involved in gamma-poly-glutamic acid synthesis. Biosci Biotechnol Biochem 73(9):2096–2102. https://doi:10.1271/bbb.90341

24. Omer BS, Pollak S, Hizi D, Eldar A (2015) The RapP-PhrP quorum-sensing system of *Bacillus subtilis* strain NCIB3610 affects biofilm formation through multiple targets, due to an atypical signal-insensitive allele of RapP. J Bacteriol 197(3):592–602. https://doi:10.1128/JB.02382-14
25. Rusnak F, Mertz P (2000) Calcineurin: form and function. Physio Rev 80(4):1483–1521. https://10.1152/physrev.2000.80.4.1483
26. Scoffone V, Dondi D, Biino G, Borghese G, Pasini D, Galizzi A, Calvio C (2013) Knockout of pgdS and ggt genes improves γ-PGA yield in *B. subtilis*. Biotechnol Bioeng 110(7):2006–2012. https://doi:10.1002/bit.24846
27. Sha Y, Sun T, Qiu Y, Zhu Y, Zhan Y, Zhang Y, Xu Z, Li S, Feng X, Xu H (2019a) Investigation of glutamate dependence mechanism for poly-γ-glutamic acid production in *Bacillus subtilis* on the basis of transcriptome analysis. J Agric Food Chem 67(22):6263–6274. https://doi:10.1021/acs.jafc.9b01755
28. Sha Y, Zhang Y, Qiu Y, Xu Z, Li S, Feng X, Wang M, Xu H (2019b) Efficient biosynthesis of low-molecular-weight poly-γ-glutamic acid by stable overexpression of PgdS hydrolase in *Bacillus amyloliquefaciens* NB. J Agric Food Chem 67(1):282–290. https://doi:10.1021/acs.jafc.8b05485
29. Shih IL, Van Y (2001) The production of poly-(gamma-glutamic acid) from microorganisms and its various applications. Bioresour Technol 79(3):207–225. https://doi:10.1016/s0960-8524(01)00074-8
30. Stanley NR, Lazazzera B (2005) Defining the genetic differences between wild and domestic strains of *Bacillus subtilis* that affect poly-gamma-dl-glutamic acid production and biofilm formation. Mol Microbiol 57(4):1143–1158. https://doi:10.1111/j.1365-2958.2005.04746.x
31. Su Y, Li X, Liu Q, Hou Z, Zhu X, Guo X, Ling P (2010) Improved poly-gamma-glutamic acid production by chromosomal integration of the *Vitreoscilla hemoglobin* gene (vgb) in Bacillus subtilis. Bioresour Technol 101(12):4733–4736. https://doi:10.1016/j.biortech.2010.01.128
32. Tomsho JW, Moran RG, Coward JK (2008) Concentration-dependent processivity of multiple glutamate ligations catalyzed by folyl poly-gamma-glutamate synthetase. Biochemistry 47(34):9040–9050. https://doi:10.1021/bi800406w
33. Tran LS, Nagai T, Itoh Y (2000) Divergent structure of the Com QXPA quorum-sensing components: molecular basis of strain-specific communication mechanism in *Bacillus subtilis*. Mol Microbiol 37(5):1159–1171. https://doi:10.1046/j.1365-2958.2000.02069.x
34. Yamaguchi F, Ogawa Y, Kikuchi M, Yuasa K, Motai H (1996) Detection of γ-polyglutamic acid (γ-PGA) by SDS-Page. Biosci Biotechnol Biochem 60(2):255–258. https://doi:10.1271/bbb.60.255
35. Yamanaka K, Maruyama C, Takagi H, Hamano Y (2008) Epsilon-poly-L-lysine dispersity is controlled by a highly unusual nonribosomal peptide synthetase. Nat Chem Biol 4(12):766–772. https://doi:10.1038/nchembio.125
36. Zeng W, Chen G, Guo Y, Zhang B, Dong M, Wu Y, Wang J, Che Z, Liang Z (2017) Production of poly-γ-glutamic acid by a thermotolerant glutamate-independent strain and comparative analysis of the glutamate dependent difference. AMB Express 7(1):213. https://doi:10.1186/s13568-017-0512-0

37. Zhang D, Feng X, Li S, Chen F, Xu H (2012) Effects of oxygen vectors on the synthesis and molecular weight of poly (γ-glutamic acid) and the metabolic characterization of *Bacillus subtilis* NX-2. Process Biochem 47(12):2103–2109. https://doi:10.1016/j.procbio.2012.07.029

Figures

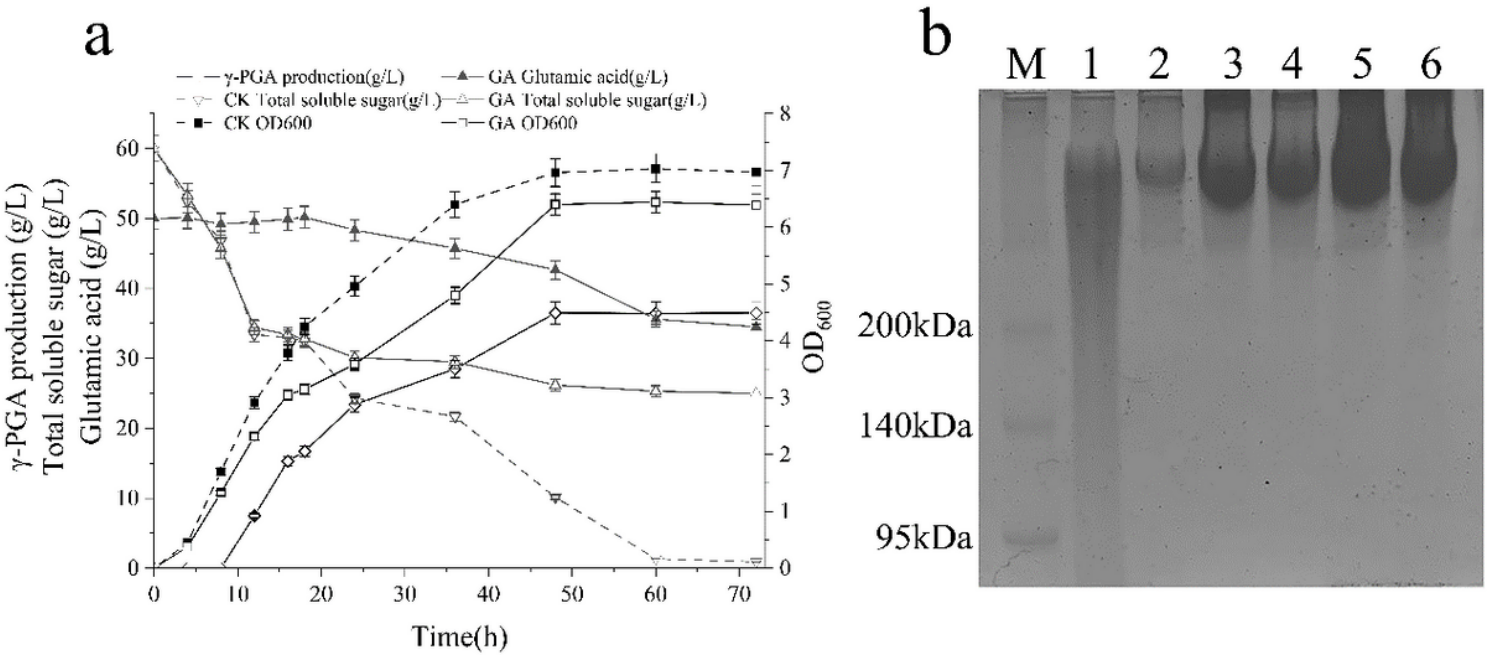

Figure 1

Changes in glucose, glutamate concentration, cell biomass, and accumulation of γ-PGA in strain SCP017-03 grown with glutamate at different fermentation times (A); SDS-PAGE analysis of γ-PGA (B), where M is a molecular weight protein marker, and lanes 1–6 are γ- PGA standard and γ-PGA samples at 20h, 36h, 48h, 60h, and 72h of fermentation, respectively.

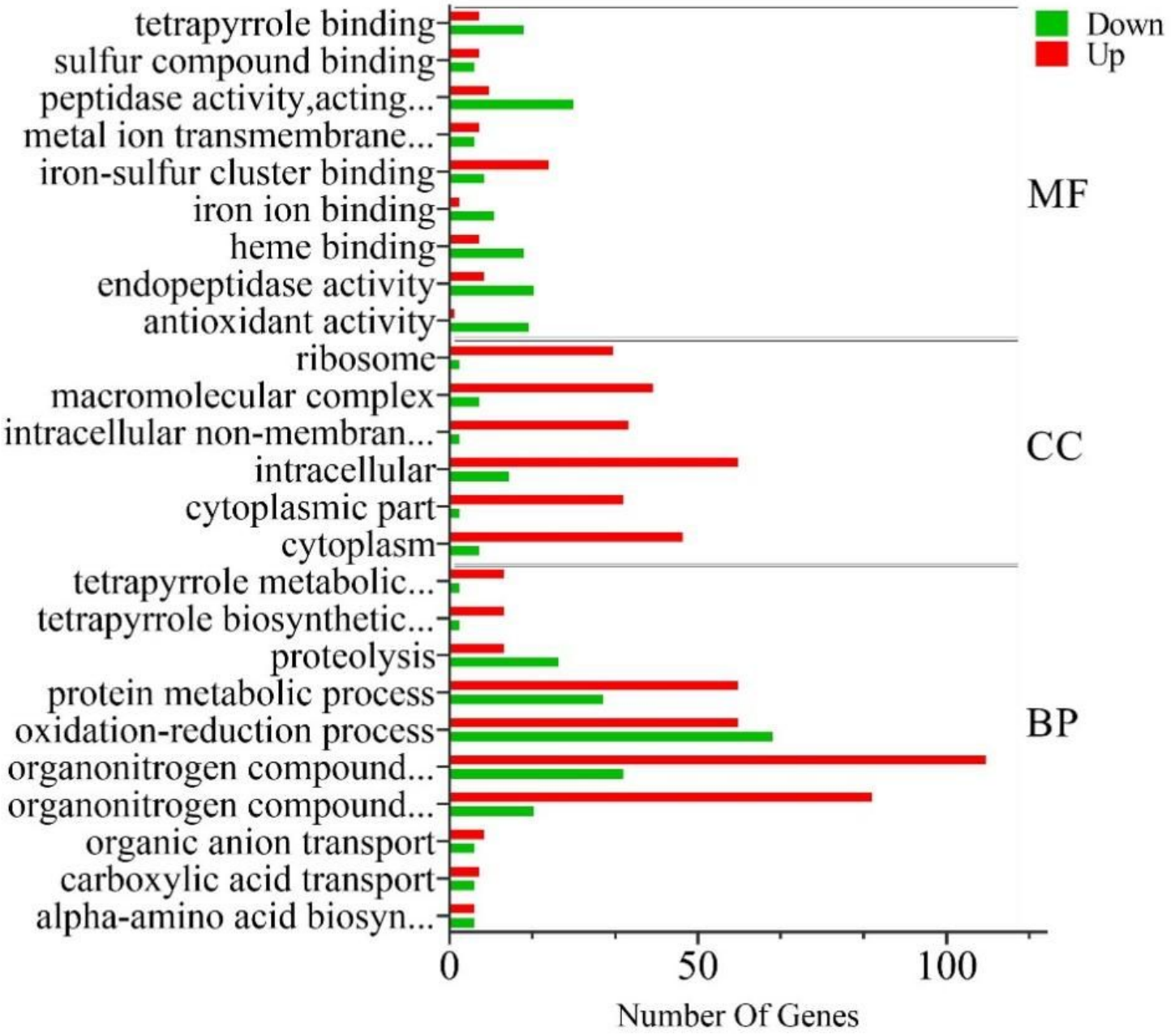

Figure 2

Bar chart illustrating GO enrichment analysis of differentially expressed genes. The horizontal axis represents the number of up-regulated and down-regulated genes in the GO Term, and the vertical axis represents the GO Term. Green indicates a downward adjustment, whereas red indicates an upward adjustment.

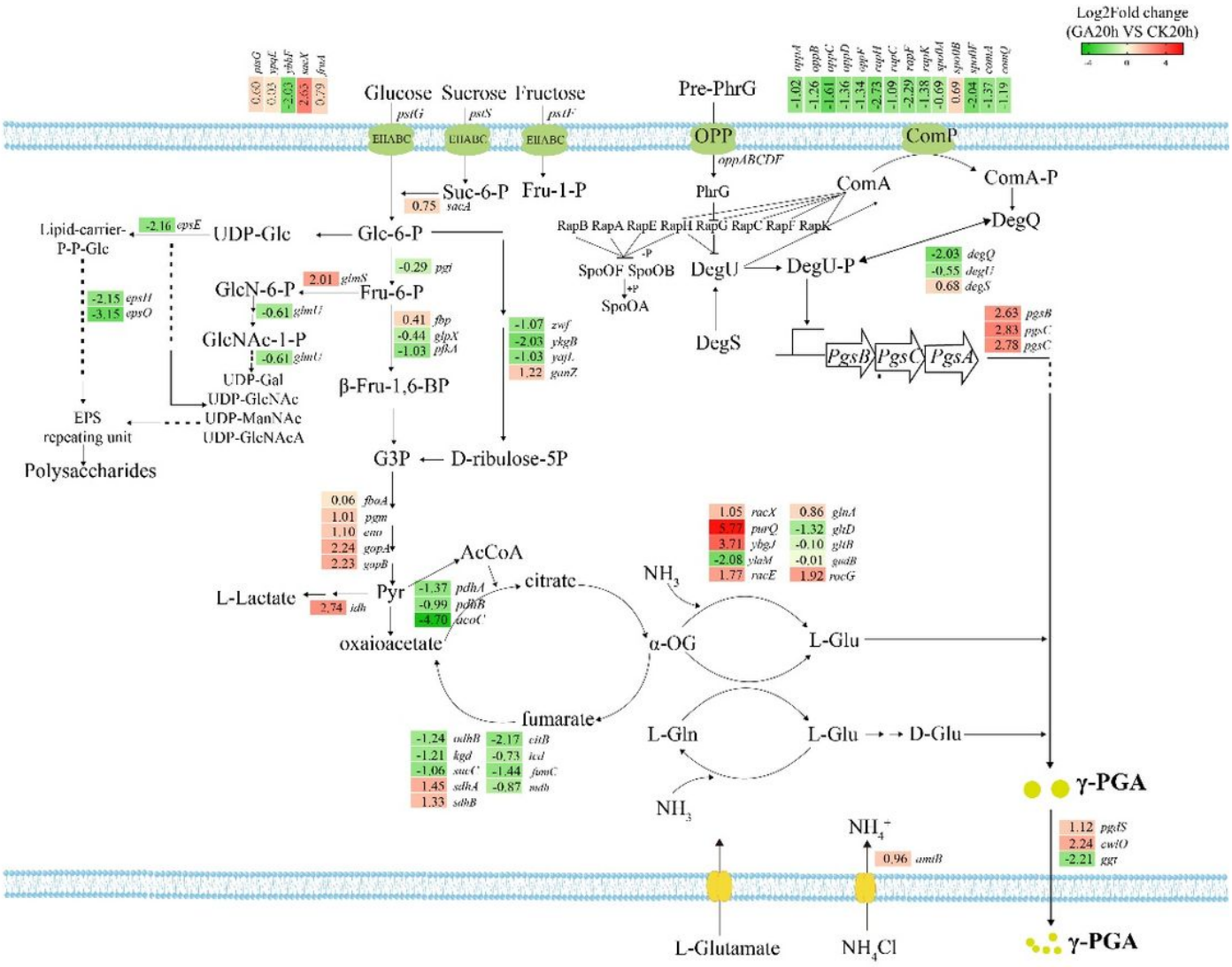

Figure 3

Transcription profiles of key genes involved in glycolysis, PPP, TCA cycle, glutamate synthesis, and γ-PGA synthesis in strain SCP017-03 grown with and without glutamate. Numbers represent expression ratios (log_2). Red indicates up-regulation, and green indicates down-regulation. Definitions: *ptsG*, *ypqE*, *ybbF*, *sacX*, and *fruA* encode phosphotransferase system; *sacA* encodes sucrose-6-phosphate hydrolase; *epsE*, *epsH*, and *epsO* encode glycosyltransferase; *glmS* encodes glutamine-fructose-6-phosphate transaminase; *glmU* encodes glucosamine-1-phosphate N-acetyltransferase; *pgi* encodes glucose-6-phosphate isomerase; *fbp* encodes Fur-regulated basic protein FbpA; *glpX* encodes bacterial fructose-1,6-bisphosphatase; *pfkA* encodes 6-phosphofructokinase; *zwf* encodes glucose-6-phosphate dehydrogenase; *ykgB* encodes 6-phosphogluconolactonase; *yajL* encodes NADP-dependent phosphogluconate dehydrogenase; *ganZ* encodes decarboxylating NADP(+)-dependent phosphogluconate dehydrogenase; *fbaA* encodes fructose-bisphosphate aldolase; *pgm* encodes phosphoglyceromutase; *eno* encodes phosphopyruvate hydratase; *gapA* and *gapB* encode glyceraldehyde-3-phosphate dehydrogenase; *idh* encodes L-lactate dehydrogenase; *pdhA* encodes E1α subunit of pyruvate dehydrogenase; *pdhB* encodes E1β subunit of pyruvate dehydrogenase; *acoC* and

odhB encodes 2-oxoacid dehydrogenases acyltransferase; *kgd* encodes alpha-ketoglutarate decarboxylase; *sucC* encodes succinyl-CoA synthetase subunit beta; *sdhA* encodes succinate dehydrogenase; *citB* encodes aconitate hydratase; *icd* encodes isocitrate dehydrogenase; *fumC* encodes fumarate hydratase; *mdh* encodes malate dehydrogenase; *racX* encodes broad specificity amino-acid racemase RacX; *purQ* encodes phosphoribosylformylglycinamidine synthase subunit PurQ; *ybgJ* encodes glutaminas; *ylaM* encodes glutaminase A; *racE* encodes glutamate racemase; *glnA* encodes type I glutamate–ammonia ligase; *gltD* encodes glutamate synthase small subunit; *gltB* encodes glutamate synthase large subunit; *gudB* encodes cryptic glutamate dehydrogenase (GDH); *rocG* encodes glutamate dehydrogenase (GDH); *DegQ* encodes pleiotropic regulator; *DegU* encodes two-component response regulator; *DegS* encodes two-component sensor histidine kinase; *pgsB*, *pgsC*, and *pgsA* encode γ-PGA synthetase operon; *comA* encodes two-component system response regulator ComA; *comP* encodes two-component system response regulator ComP; *oppABCDF* encode oligopeptide ABC transporter substrate-binding protein; *rapHCFK* encode response regulator aspartate phosphatase; *spo0ABF* transcription factor Spo0A; and *spo0BF* encode sporulation initiation phosphotransferase Spo0F.

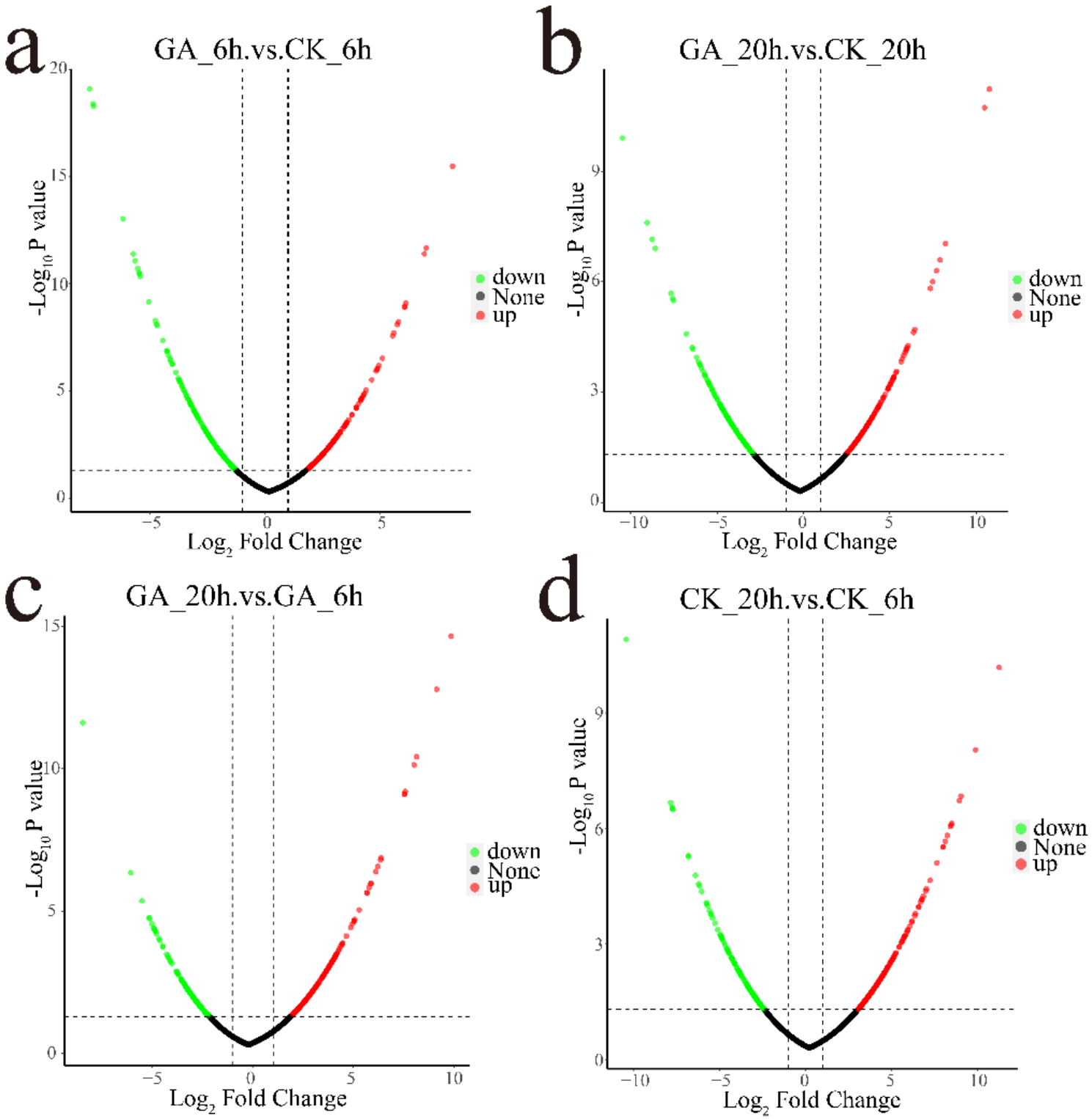

Figure 4

Volcano plots depicting differential protein expression. A: Comparison of protein levels between strains with and without glutamate at the 6th hour of fermentation. B: Comparison of protein levels between strains with and without glutamate at the 20th hour. C: Comparison of protein levels between strains at the 20th and 6th hours of fermentation with glutamate. D: Comparison of protein levels between strains at the 20th and 6th hours of fermentation without glutamate. The horizontal axis represents the multiple

differences (log_2 value) of differentially expressed proteins, and the vertical axis represents the P_{value} (-log_{10} value). Black represents proteins with insignificant differences, red represents significantly up-regulated proteins, and green represents significantly down-regulated proteins.

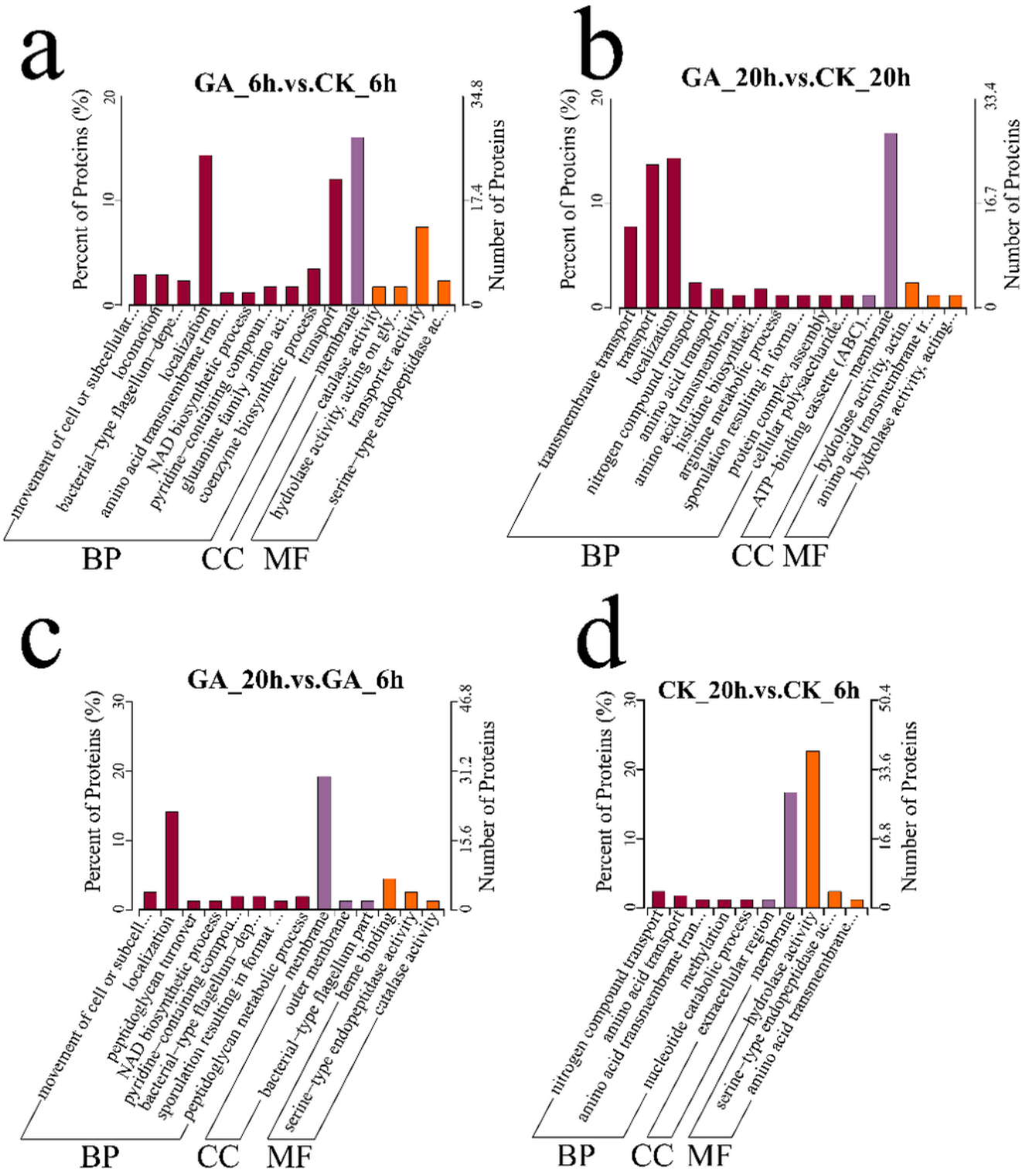

Figure 5

Statistical diagram of GO secondary annotation classification for differentially expressed proteins. A: Differential protein GO enrichment of strains with and without glutamate at the 6th hour of fermentation. B: Differential protein GO enrichment of strains with and without glutamate at the 20th hour of fermentation. C: Differential protein GO enrichment of the strain at the 20th and 6th hours of fermentation with glutamate. D: Differential protein GO enrichment at the 20th and 6th hours of fermentation without glutamate. The horizontal axis represents GO entries enriched with differential proteins, and the vertical axis represents the number of differentially expressed proteins annotated to a certain GO entry.

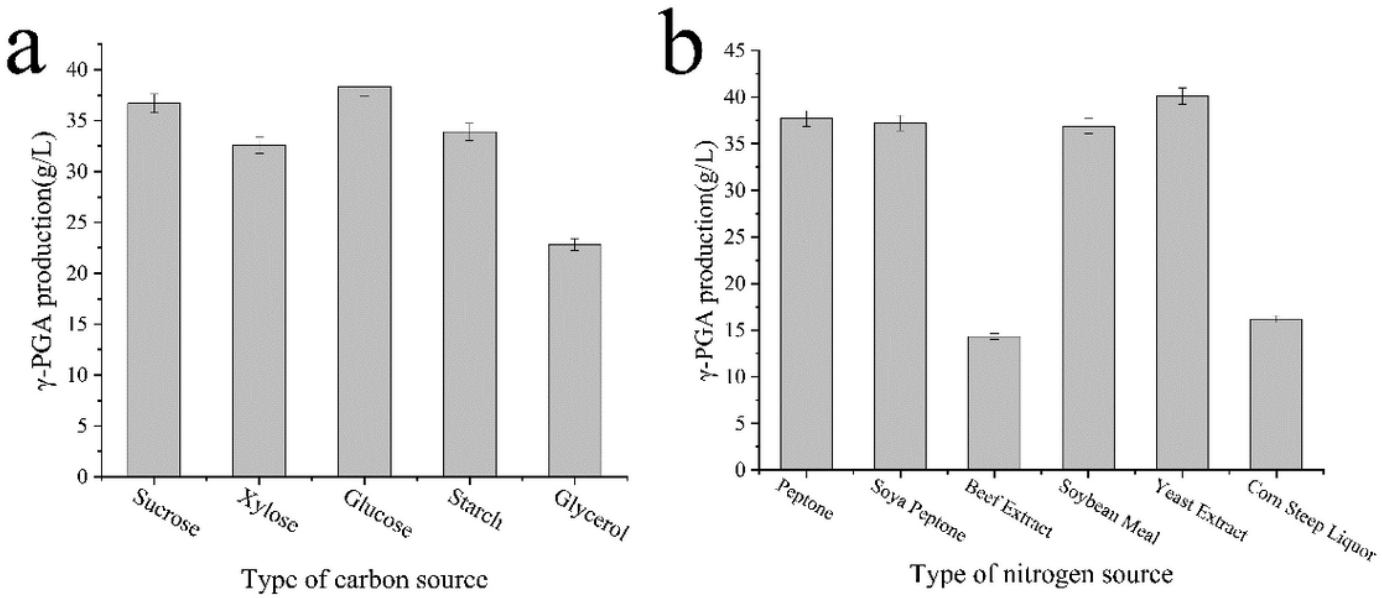

Figure 6

Effects of different carbon (A) and nitrogen sources on the yield of γ- PGA (B).

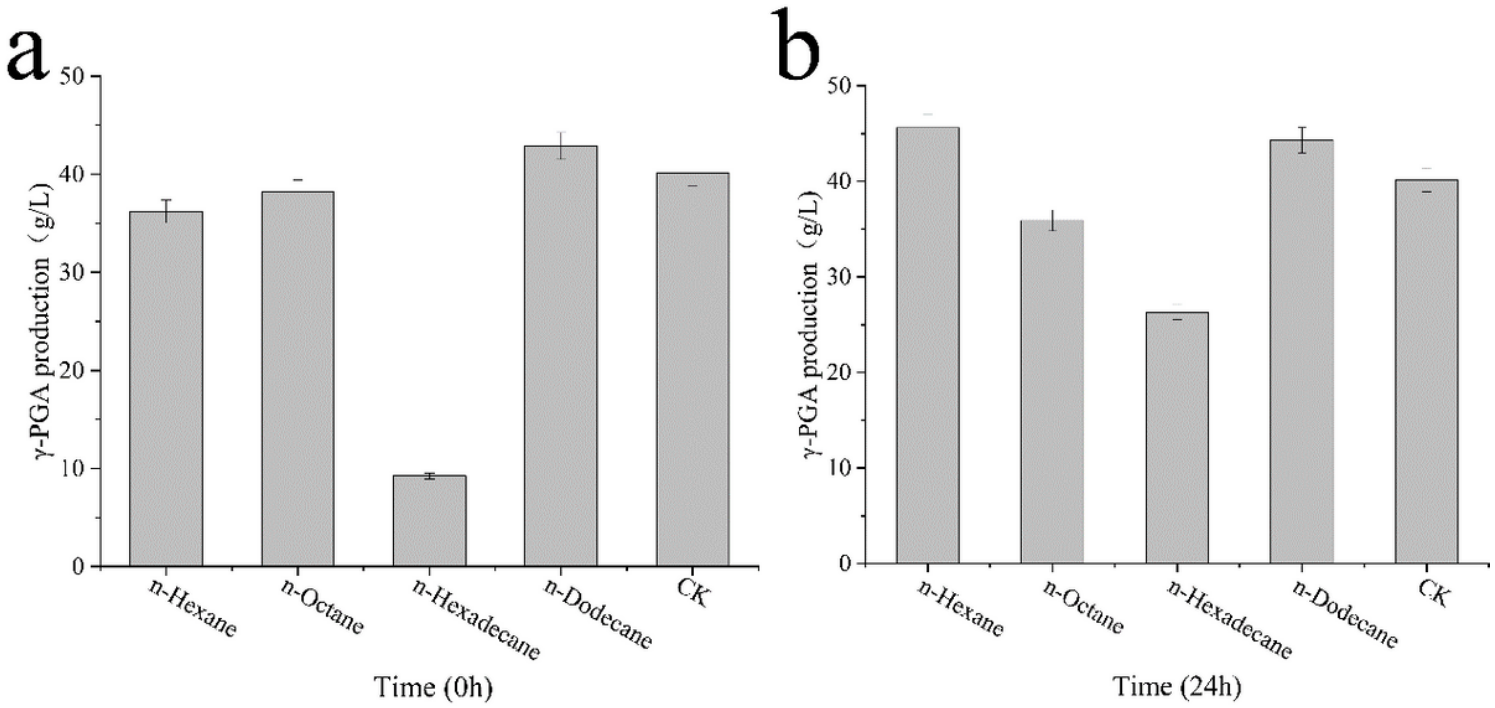

Figure 7

Effects of different organic oxygen carriers (A) and their addition time (B) on the yield of γ- PGA.

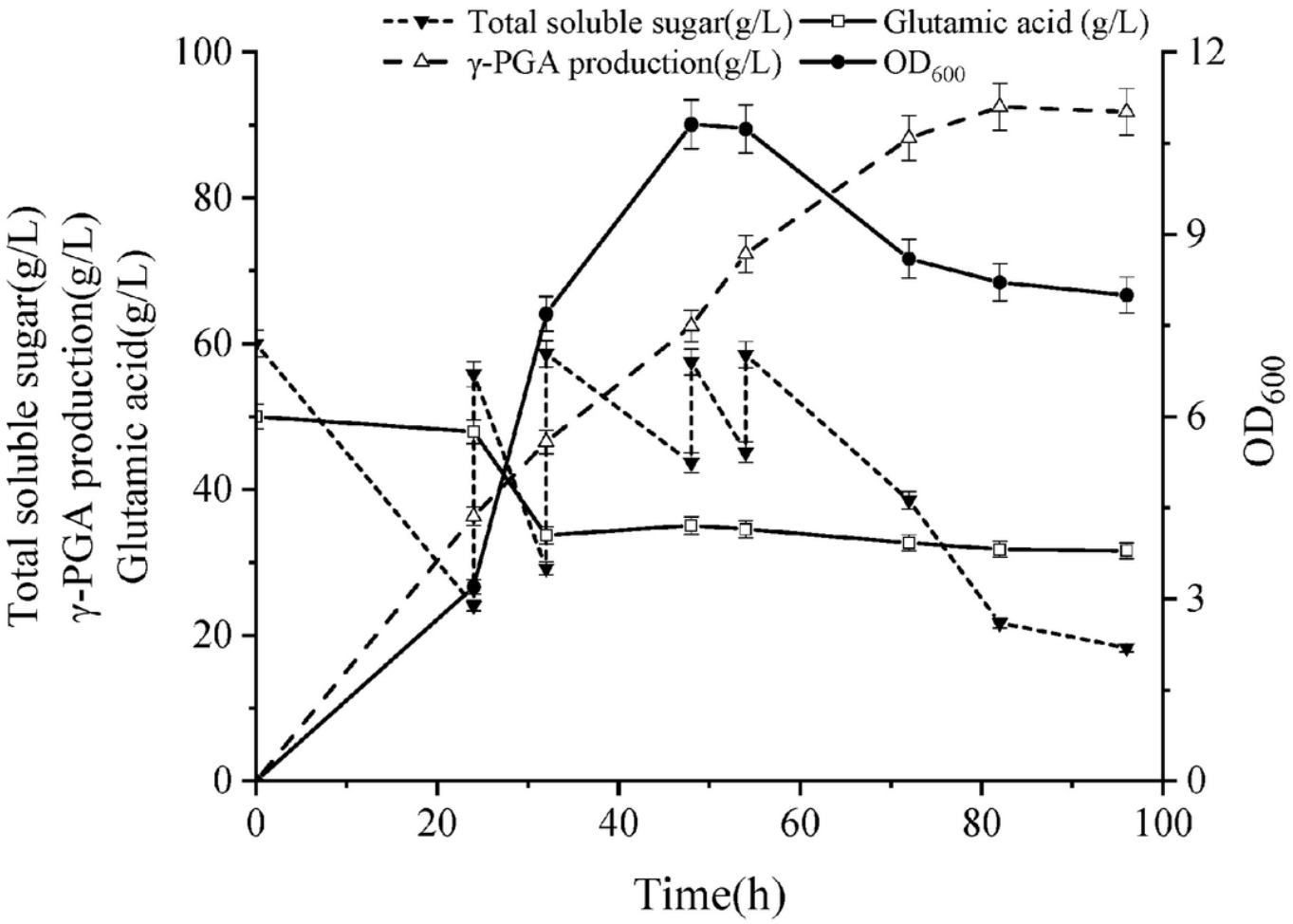

Figure 8

Changes of glucose, glutamate concentration, and cell biomass during the production of γ-PGA in 5L fed-batch fermentation.

Supplementary Files

This is a list of supplementary files associated with this preprint. Click to download.

- TableS1..xlsx
- TableS2..xlsx